Proceedings of the XVII ECSMGE-2019
Geotechnical Engineering foundation of the future
ISBN 978-9935-9436-1-3

doi: 10.32075/17ECSMGE-2019-0789

XVII European Conference
ECSMGE 2019
Reykjavik
on Soil Mechanics
and Geotechnical Engineering

Flood performance of earth embankments

Performances de terres de remblai

J. A. Black
University of Sheffield, Sheffield, United Kingdom

I.U. Khan
University of Sheffield, Sheffield, United Kingdom

K. Nakashima, Y. Nakata
Yamaguchi University, Ube, Japan

ABSTRACT: Earth embankment structures are vital to protect against flooding and their failure can result in significant loss of life and infrastructure damage. The increasing frequency of flood events requires defences to be able to withstand multiple flood loading scenarios where excess pore water pressures within the embankment can lead to local instability of a full breach. Centrifuge model tests of a 1:30 scaled embankment subjected to multiple flood events with a final overtopping phase to evaluate resilience is presented. A tension crack along the embankment crest on the waterside was observed after dissipation of the first flood water which proved critical to the overall stability of under repeated cycles. Overtopping was shown to initiate significant surface erosion on the landside slope that lead to full breaching of the structure.

RÉSUMÉ: Les structures de remblais en terre sont vitales pour la protection contre les inondations et leur défaillance peut entraîner des pertes de vie et des dommages d'infrastructure importants. La fréquence croissante des inondations oblige les défenses à être en mesure de résister à de multiples scénarios de charge d'inondation dans lesquels des pressions d'eau excessives dans les pores du talus peuvent conduire à une instabilité locale d'une brèche totale. Les essais sur modèle en centrifugeuse d'une terre de remblai à l'échelle 1:30 soumis à de multiples inondations avec une phase finale de débordement pour évaluer la résilience sont présentés. Une fissure de tension le long de la crête du remblai au bord de l'eau a été observée après la dissipation des premières eaux de crue, ce qui s'est avéré essentiel pour la stabilité globale des cycles sous-répétés. Il a été démontré que les retombées provoquent une érosion de surface importante sur la pente côté terre qui conduit à une rupture complète de la structure.

Keywords: flood, embankment, erosion, centrifuge

1 INTRODUCTION

Earth embankment structures are often used to protect from flooding. Past disasters and the increased frequency of devastating flood events have triggered many governments around the globe to invest in comprehensive flood risk management initiatives such as flood control schemes, early warning systems and evacuation planning. Despite their apparent simplicity, earth embankments can be surprisingly complex structures. Often constructed from locally won fill material, their construction can often be highly irregular in nature with poor historical records kept. Breaches of flood defences can

result in significant economic loss, as witnessed in the summer of 2007 in the UK where flood damage was estimated at £3.1 billion (Defra, 2008).

Increased pore water pressure within flood embankments can result in stability and failure via several modes: (*i*) deep-seated slope instability due to soft clay founding layers; (*ii*) piping due to excessive uplift pressures in underlying layers; (*iii*) internal erosion; and (*iv*) erosion of either the outward (waterside) and landward (landside) face due to standing water or overtopping. The hydraulics associated with flood embankments should be carefully considered during the design in order to identify and minimise risk. Pore water pressures can fluctuate enormously from natural low background levels to those established during extreme flood events, the frequency and magnitude of which are increasing during operational life. These fluctuations can result in softening of the embankment slopes leading to local instability that can lead to a full breach of the flood defence.

The method of centrifugal modelling of hydraulic structures has been successfully utilised to investigate the performance of dams, embankments, dikes etc. (Hudacsek et al., 2009). Benefiting from the accelerated time scaling of seepage diffusion processes; observations that would typically require several weeks in a large 1*g* model can be achieved in a centrifuge model test within a few hours. This offers significant opportunity to evaluate the performance of flood embankments subjected to flooding in a reduced timescale. The work presented in this paper reports on the performance of a centrifuge model test embankment subjected to four flood cycles, followed by overtopping; to investigate the impact of cyclic pore water pressure changes on stability and breaching.

2 EXPERIMENTAL STUDY

Understanding the deterioration and damage to embankment flood protection systems under repeated flooding is vital to improve resilience against extreme weather events. The following sections describe the physical model, soil conditions, and details of the experiments undertaken.

2.1 Experimental programme

A 1:30 scale model flood embankment was tested on the University of Sheffield 4m diameter geotechnical beam centrifuge at 30 times Earth's gravity ($N = 30g$) (Black et al., 2014). A plane strain box having internal dimensions 0.6m (L) x 0.2m (W) x 0.4m (H) was used. The box incorporated a viewing window to capture images for digital image correlation (DIC). Flooding was achieved by porting water over the main centrifuge hydraulic fluid union to the test package in-flight with local control on the package enabled by a water distribution plate (Khan et al., 2018). Flood water was triggered and dissipated using a series of solenoid and proportional valves integrated into the main water supply line and the discharge drainage channels of the test box. The prototype embankment modelled had a geometry of 5 m high, 3 m crest width, base of 13 m with a slope 1:1. Details of the experiment configuration and shown in Figure 1.

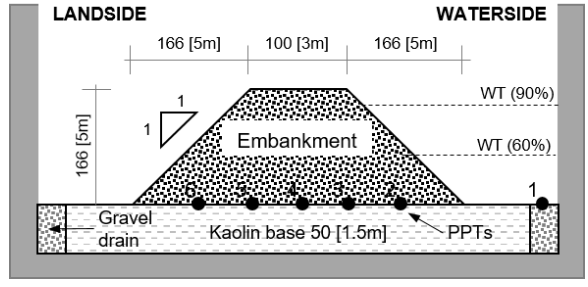

Figure 1. Summary of the model embankment

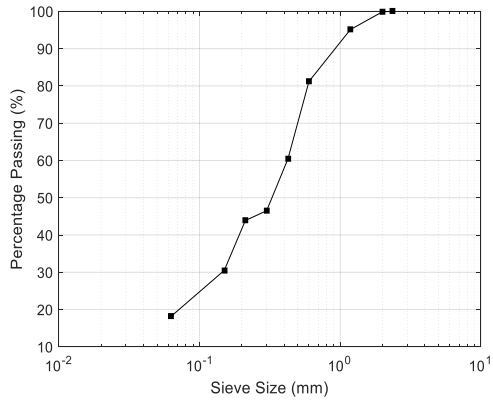

Figure 2. Partlicle size distribution

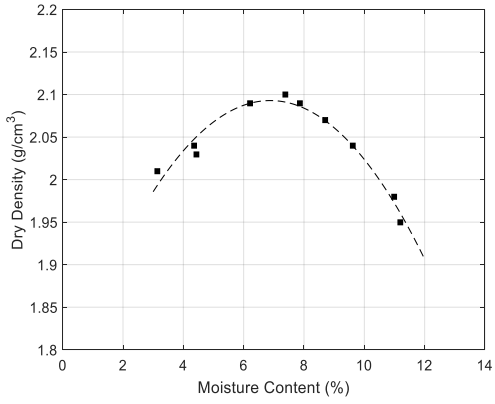

Figure 3. Compaction curve

2.2 Experimental materials

A well graded soil was used for this study which incorporated fine and coarse grain fractions. Table 1 outlines the soil materials that were blended to create the soil mix for this investigation. The combined particle size distribution curve is shown in Figure 2. This material was carefully engineered to minimise the potiential of internal erosion. Susceptibility of internal erosion was checked according to the procedures outlined by Skempton and Brogan (1994) and the current material was determined to have an H/F ratio in excess of 1.3, thus is confirmed to be stable. This was important to ensure that any instability observed could be attributed to seepage flow/pore water pressure effects and not changes in soil grading by internal erosion; which typically requires longer sustained seepage flow to manifest compared to instability by rapid changes in pore water pressure generated by flooding.

Table 1. Soil mix ratio.

Material	Percentage (%)
SAND - CH30	10.5
SAND - HST95	26
SAND - LBS Fraction A	5
SAND - LBS Fraction B	13.5
SAND - LBS Fraction C	27
SILT	8
CLAY – Kaolin	10

2.3 Model preparation

The embankment was constructed by compaction. A preliminary investigation was undertaken to determine the moisture content – density characteristics of the soil. Figure 3 indicates a maximum dry density of 2.1 g/cm^3 at a moisture content of 7 %. A clay base (kaolin) was compacted at a moisture content of 13 % into the centrifuge test box up to a height of 50 mm. This provided a low permeable layer (k = 1x10^{-9} m/s) which ensured that the seepage flow would be predominantly through the higher permeability embankment material (k = 1x10^{-7} m/s); not under it so as to cause piping or boiling at the toe on the landside slope.

Once the surface of the base clay layer was flattened, several tracks were cut to enable 5 pore water pressure sensors to be placed in the base of the embankment (PPT-2 to PPT-6). A 6th sensor (PPT-1) was located next to the waterside embankment slope to record the flood water driving head (Figure 4a). Prior to placement the sensors were saturated to ensure that any pore pressure changes would be recorded quickly and not delayed due to rehydration of the sensor filters. The surface of the clay was keyed and a further 4 layers, each 50mm thick, of the embankment soil mixture at a moisture content of 7.5 %, were compacted in place (Figure 4b). A

2.5 kg drop hammer was used with 50 blows applied per layer to create a firm soil block from which the embankment would be sculpted (Figure 4c). The sides of the centrifuge strong box were lightly greased to minimise frictional boundary effects with texture being added to the front window that would enable DIC tracking of soil movements of the embankment with each flood cycle. Note, once the soil was compacted into the test chamber the side plates were not removed as stress relief of the material could create preferential drainage paths along the interface boundary. The soil was profiled to the geometry as indicated in the schematic diagram (Figure 1), using pallet knives and several guide plates.

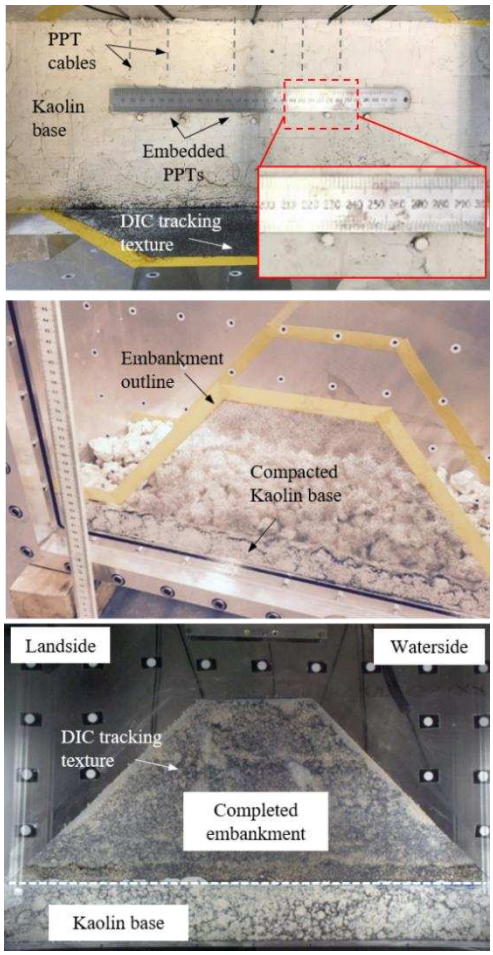

Figure 4. Sample preparation

Once the embankment was trimmed, a gravel drain was installed at each end of the test chamber which allowed free draining end conditions. A fine mesh was used to separate the clay base from the drains to prevent clogging. The model was then transferred to the centrifuge platform, instrumentation sensors connected to the data acquisition and the camera systems configured for DIC measurement. A Basler Pilot pia2400 5MP camera was interfaced with a LabVIEW Virtual Instrument (VI) controller to automatically capture images during the test every 10 seconds to provide an episodic account during each flood event.

2.4 Test procedures

The model was accelerated to 30*g*, at the effective radius of 1.9 m, and held for a period of 15 minutes. This stage was implemented to allow re-compression of the embankment under increased self-weight stresses and initialisation of internal pore water pressures. The embankment was then subjected to flooding on the waterside. A two stage flood process was observed, initially a flood representing 50 % of the embankment height occurred in 120 seconds and was sustained for a total of 672 seconds; followed by further flooding up to 90 % of the embankment height, also sustained for 672 seconds. In each case this corresponded to a prototype flood time of 30 hours, sustained for 168 hours (7 days). The flood was removed and the elevated pore water pressure allowed to dissipate for 14 days before repeating with 2 further flooding cycles (3 in total). A final flood event (4th cycle) increased immediately to 90% height in a prototype equivalent of 2.2 days and was maintained for 18 days, at which point the flood level was increased so as to overtop the embankment.

3 RESULTS

The following sections outline the salient observations of the embankment performance in relation to the internal pore water pressure

response recorded and displacement/strain observations from the DIC image analysis. Matlab and GeoPIV (White et al., 2003) were used to compute the DIC analysis.

3.1 Hydraulic response to 1st flood event

The hydraulic response to the initial flood event up to 50 % and then 90 % of the embankment height is shown in Figure 5, presented as pressure head. The flood level on the waterside of the embankment is depicted by PPT-1 with other internal pore pressure measurements indicated by PPT-2 to PPT-6, noting that PPT-2 is closest to the waterside with PPT-6 furthest toward the landside. A clear delay in pore pressure response is observed due to the time required for the elevated waterside pressure head to infiltrate and flow through the embankment. PPT-2 closely follows PPT-1, with PPT-3 to PPT-5 rising gradually with prolonged seepage duration. PPT-6 remains relatively unchanged confirming the excess pore pressure dissipates before reaching the landslide slope. Once the flood water recedes, there is a time lag before the peak pressures are recorded internally at other sensor locations, before a gradually reducing. The latter point is important to note when reflecting on the performance/factor of safety of the earth embankment structure as the minimum internal effective stress, and hence the most critical conditions, are likely to occur after the original flood waters being to dissapite.

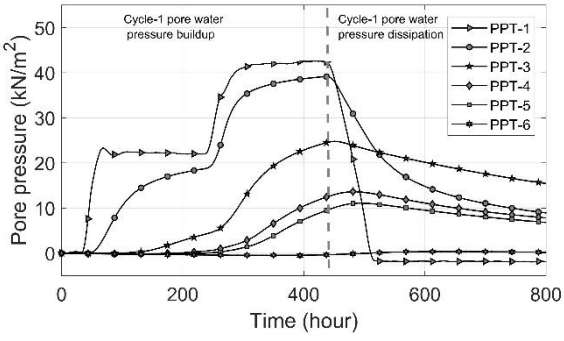

Figure 5. Pore pressure response in cycle 1

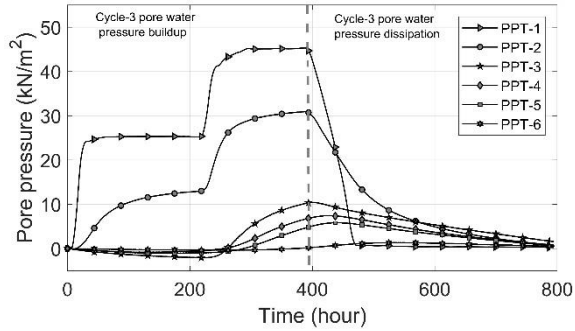

Figure 6. Pore pressure response in cycle 3

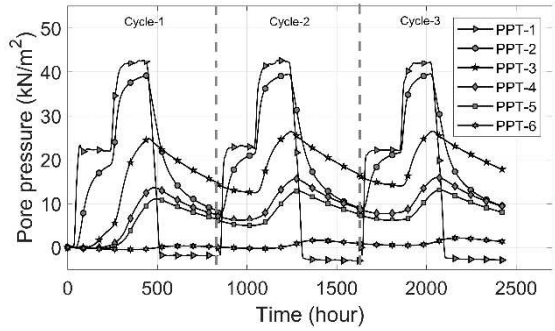

Figure 7. Pore pressure during repeat flooding

3.2 Hydraulic response to 2nd and 3rd flood cycles

The internal hydraulic performance in flood cycle 2 and 3 is typified in Figure 6. Observations reflect those made in the 1st flood event with respect to the delay in pore pressure generation across the embankment structure and the peak values achieved. Note that in Figure 6 the data has been zeroed at the onset of the flood event, hence the pressures shown reflect only the change in head. In the early stages of the flooding it is interesting to note that reductions in pore pressure are observed in PPT-3 to PPT-6 up to 200 hours; reflecting that the new pressure head from the incoming flood had not infiltrated the embankment to this point and the effects of pressure head dissipation from the previous flood history were still ongoing. This process is clearly evident in Figure 7 which presents an episodic account of the total pore water pressures recorded from the start of flood 1 to end of the 3rd flood cycle. While there is a reduction in pore pressure

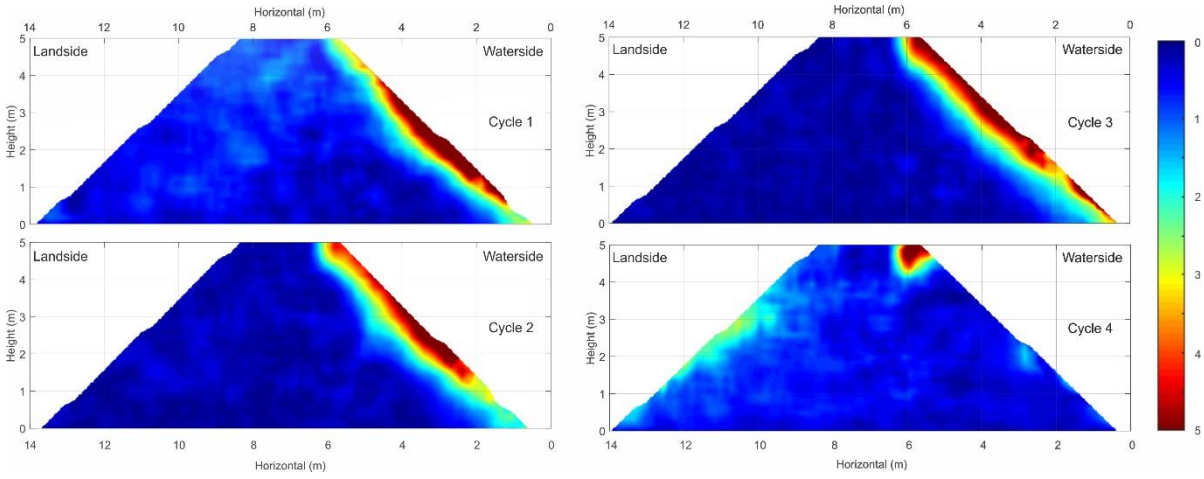

Figure 8. Resultant soil displacements after each flood cycle

before responding to the new flood event; it is notable that a general increase in background pore water pressure can be seen within the core of the embankment with each cycle (*i.e.* traces of PPT-3 to PPT-6 where an increase in pressure head equivalent to a 0.5 m shift in the water table occurred.

While this increase is a function of the time separation between flood events in the current experimental programme; it serves as a timely reminder that multiple flood events occurring in quick succession in reality could have catastrophic consequences on embankment stability in periods of heavy or continual rain/flooding where background pore water pressure increases could occur. Similar effects would also be observed if drainage channels were blocked by fines or became less effective with time.

3.3 DIC observations cycle 1 to 3

Images captured during the flood events were used to determine movement of the embankment. The resultant displacements are plotted in Figure 8 for each flood cycle with the maximum magnitude of 5 mm shown for direct comparison.

During the initial flood cycle softening of the waterside slope occurred that, upon dissipation of the flood water, led to movements on the slope surface toward to the toe position. After the 2nd flood cycle movements were seen to propagate along the slope toward the crest position. A large tension crack formed in upper surface of the crest corresponding to the intercept of the waterside slope movements (Figure 9). Image analysis determined the crack to be 0.9 m deep. When the water level increased from 50 % to 90 %, the tension crack was observed to partially close due to the increased hydrostatic stresses imposed by the water translating lateral thrust on the embankment. However, as the flood water receded the crack re-opened, growing in depth and width, triggering a sliding mechanism parallel to the slope surface.

3.4 Overtopping

A final flood event (4th cycle) was increased immediately to 90 % height in 2.2 days, and was maintained for 18 days. No global failure was observed at this point; however, a small local slip was observed near the toe of the landslide slope. Pore water pressures at PPT-6 increased to 10 kN/m^2 in this phase which triggered this local instability (Figure 10). Higher levels of pore pressure were recorded across the embankment indicating that the longer flood duration at 90 %

was critical to the stability of the landslide slope as shorter duration events did not yield local failure.

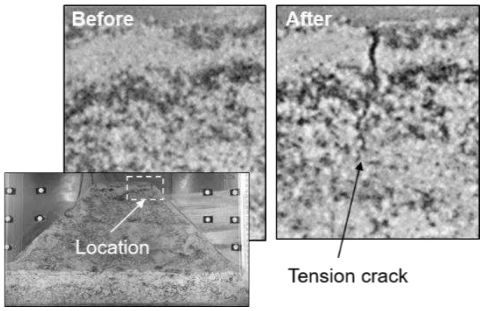

Figure 9. Tension crack developing

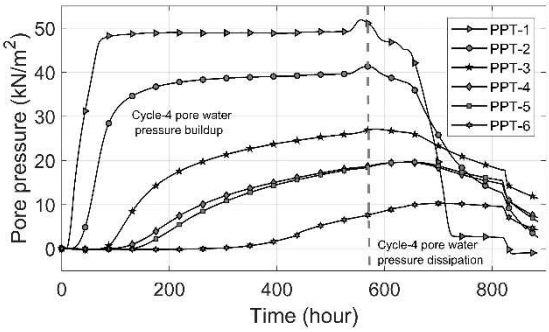

Figure 10. Pore pressure response in cycle 4 and overtopping

The flood level was increased so as to overtop the embankment to explore the consequences on global stability. This proved critical to the integrity of the embankment structure as flood water was able to enter the embankment from the top surface. The surface soil fluidised and eroded freely from landside slope and heart of the embankment that caused catastrophic failure. Evidence of this can be seen landside movement is shown in Figure 8, cycle 4 and by images of the failed embankment (Figure 11). Larger local movements were also observed in the location of the initial tension crack which slumped considerably on termination of the flood. This confirms the need for surface erosion protection measures on earth embankments, but also the need to investigate resilience for both static floods and rainfall infiltration which could present similar effects as a full overtopping event.

4 CONCLUSIONS

The work presented in the paper focused on the cyclic stability of an earth embankment subjected to multiple flood events. Softening and subsequent movement of the waterside slope ocurred during the initial flood phases that lead to downward movement parallel to the slope that ratcheted from the toe toward the crest. Increased movement occurred with each cycle which lead to the formation of a tension crack probigating 0.9m from the crest into the embankment. Progressive deepening and widening of this crack occurred as the hydrostatic flood pressure increased and reduced. The crack led to the a shear region forming parallel to the slope. Sustained flooding of 90 % lead to rapid increase in the internal pore pressures across the embankment. This triggered local instability of the landslide slope at the toe due to excess pore pressures generation reducing the effective stress. Overtopping of the embankment had disasterious consequences for the embankment. Significant surface erosion of thte landside slope occurred and a large eroided channel formed through the centre of the embankment. This confirms that vegitation or surface protection is vital to prevent catastrophic failure should overtoping occur.

5 ACKNOWLEDGEMENTS

Funding support provided by the Engineering Physical Sciences Research Council (EPSRC) to establish the 4 m diameter beam centrifuge and Centre for Energy and Infrastructure Ground Research at the University of Sheffield is gratefully acknowledged. This work was enabled through Yamaguchi University student placement funds.

6 REFERENCES

Black, J.A., Baker, N., Ainsworth, A., 2014. Establishing a 50 g-ton geotechnical centrifuge at the University of Sheffield. *Proceedings of the 8th International Conference on Physical Modelling in Geotechnics*.

Defra, 2008. A Framework for pro-environmental behaviours. *Department for Environment, Food and Rural Affairs, London*.

Hudacsek P., Bransby M.F., Hallett P. D., Bengough A. G., 2009. Centrifuge modelling of climatic effects on clay embankments Proceedings of the Institution of Civil Engineers: Engineering Sustainability **162**(2), 91-100.

Khan, I.U., Al-Fergani, M., Black, J.A., 2018. Developing a rainfall simulator for climate modelling. *Proceedings of the 8th International Conference on Physical Modelling in Geotechnics*.

Skempton, A.W., Brogan, J.M., 1994. Experiments on piping in sandy gravels. *Géotechnique* **44**(3), 449-460.

White, D., Take, W., Bolton, M., 2003. Soil Deformation Measurement Using Particle Image Velocimetry (PIV) and Photogrammetry, *Géotechnique* **53**(7), 619–631.

.